# Pulse-Encoded Ultrasound Imaging of the Vitreous With an Annular Array

*Ronald H. Silverman, PhD*
*Jeffrey A. Ketterling, PhD*
*Jonathan Mamou, PhD*
*Harriet O. Lloyd, MS*
*Erwan Filoux, PhD*
*D. Jackson Coleman, MD*

## ABSTRACT

The vitreous body is nearly transparent both optically and ultrasonically. Conventional 10- to 12-MHz diagnostic ultrasound can detect vitreous inhomogeneities at high gain settings, but has limited resolution and sensitivity, especially outside the fixed focal zone near the retina. To improve visualization of faint intravitreal fluid/gel interfaces, the authors fabricated a spherically curved 20-MHz five-element annular array ultrasound transducer, implemented a synthetic-focusing algorithm to extend the depth-of-field, and used a pulse-encoding strategy to increase sensitivity. The authors evaluated a human subject with a recent posterior vitreous detachment and compared the annular array with conventional 10-MHz ultrasound and spectral-domain optical coherence tomography. With synthetic focusing and chirp pulse-encoding, the array allowed visualization of the formed and fluid components of the vitreous with improved sensitivity and resolution compared with the conventional B-scan. Although optical coherence tomography allowed assessment of the posterior vitreoretinal interface, the ultrasound array allowed evaluation of the entire vitreous body. **[Ophthalmic Surg Lasers Imaging 2012;43:82-86.]**

## INTRODUCTION

The vitreous body is a homogeneous and optically transparent gel in the young eye. It contains macromolecules including glycosaminoglycans (primarily hyaluronan) and a collagen extracellular matrix. The vitreous cortex, a thin collagen-rich layer surrounding the vitreous body, is thin at the macula and absent over the optic disc.[1] The vitreous base, located along the ora serrata, has a dense concentration of collagen fibers and forms strong attachments with the retina.[2] The aging process and certain pathologies, such as lattice degeneration,[3] can result in tractional retinal tears and detachment. Pathologic vitreoretinal interactions may also occur in diabetic retinopathy, age-related macular degeneration, proliferative vitreoretinopathy, and macular holes.

As early as 1978, Oksala demonstrated age-related degenerative changes in the vitreous body with 6-MHz ultrasound.[4] Current 10- to 12-MHz ultrasound B-scan systems provide real-time display, enabling characterization of vitreous mobility, and can generally visualize the vitreoretinal interface and retinal traction in posterior vitreous detachment (PVD).[5-7] Although higher frequencies can improve resolution, the exponential increase in attenuation with frequency makes detection of faintly reflective fluid/gel vitreous interfaces problematic as frequency is increased.[8]

*From the Department of Ophthalmology (RHS, HOL), Columbia University Medical Center; Frederic L. Lizzi Center for Biomedical Engineering (RHS, JAK, JM, EF), Riverside Research; and Weill Medical College of Cornell University (DJC), New York, New York.*

*Originally submitted February 1, 2011. Accepted for publication August 12, 2011. Posted online September 8, 2011.*
*Supported in part by NIH grant EB008606 and an unrestricted grant to the Department of Ophthalmology, Columbia University Medical Center from Research to Prevent Blindness, Inc.*
*The authors have no financial or proprietary interest in the materials presented herein.*
*Address correspondence to Ronald H. Silverman, PhD, Department of Ophthalmology, Harkness Eye Institute, Columbia University Medical Center, 160 Ft. Washington Ave., Room 509A, New York, NY 10032. E-mail: rs3072@columbia.edu*
*doi: 10.3928/15428877-20110901-03*

The vitreoretinal interface can also be assessed using optical coherence tomography (OCT). The high speed, sensitivity, and resolution of spectral-domain OCT systems have made visualization of vitreoretinal interface readily achievable in two-dimensional[9-11] and three-dimensional images.[12] However, OCT is unable to image the vitreous body as a whole due to its limited depth-of-field and the optical opacity of intervening anterior structures, including the iris and sclera.

The limited depth-of-field of fixed-focus, single-element ultrasound probes can be improved by using multi-element probes and synthetic focusing.[13] Reduced sensitivity at higher frequencies can be addressed by using "pulse-encoded" transducer excitation.[14] We describe the first clinical application of these technologies for evaluation of a case of age-related PVD with comparative conventional ultrasound and OCT imaging.

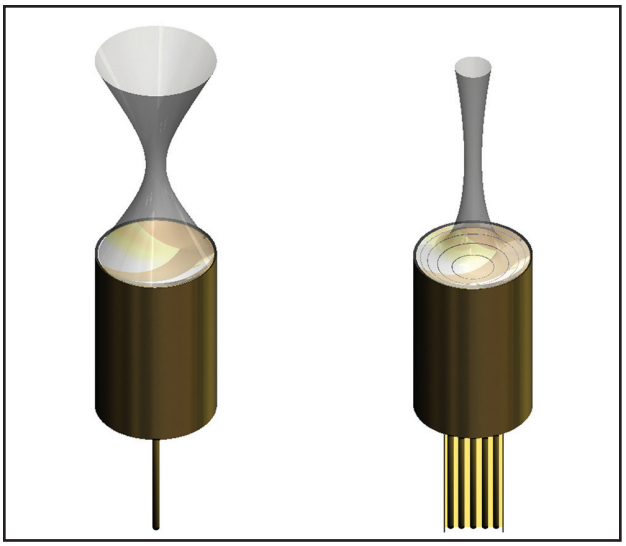

**Figure 1.** Rendering of conventional single-element (left) and prototype annular array (right) transducers and ultrasound fields. The array consists of five concentric piezopolymer elements, each of which acts successively as the emitter while all five elements receive echo data. The narrow shape of synthetically focused beam produced by the array is indicative of its increased depth-of-field compared with the single element probe where sensitivity and lateral resolution are high only near the waist of the focused beam.

## REPORT

This investigation was performed with informed consent under a protocol approved by the Institutional Review Board of the Weill Medical College of Cornell University. The five-element annular array had a 10-mm aperture with its surface spherically curved to produce a 31-mm focal length. The fabrication process has been previously described in detail.[15]

Images were formed from five consecutive scans, with each of the five elements acting in turn as the emitter while all elements received. We excited each element with a linear chirp, a sinusoidal waveform increasing in frequency with time. The chirp, 4 µsec in duration and spanning frequencies from 6.5 to 32 MHz, was generated by an arbitrary waveform generator (Model WW1281A; Tabor Electronics, Haifa, Israel) and amplified (ENI model A150; Rochester, NY) to excite the transducer. Echo data were digitized (200 MHz, 8-bits/sample, PXI-5152; National Instruments, Austin, TX) and a digital compression filter was applied to the raw echo data.[7] Synthetic focusing was then implemented by time-shifting each of the 25 digitized waveforms to simulate focusing at a series of 41 successive depths to form a final composite image.[16] Scan sets were acquired in 0.5 second and processed in approximately 1 second. Comparative renderings of a single-element transducer, the array, and their sound fields are provided in Figure 1.

Transducer output, summarized in the table, was measured for monocycle and chirp excitation modes

TABLE

**Acoustic Measurements at the Transducer Focus Compared With FDA 510k Ophthalmic Ultrasound Safety Limits[a]**

| Mode | $I_{SPPA.3}$ (W/cm$^2$) | $I_{SPTA.3}$ (mW/cm$^2$) | MI |
|---|---|---|---|
| Monocycle | 11.4 | 0.03 | 0.016 |
| Chirp | 13.0 | 0.33 | 0.019 |
| FDA 510k limit | 28 | 17 | 0.23 |

*FDA = Food and Drug Administration; $I_{SPPA.3}$ = derated spatial-peak pulse-average intensity; $I_{SPTA.3}$ = derated spatial-peak time-average intensity; MI = mechanical index.*

*[a]Values correspond to the maximum value for each measurement obtained over the 5 annuli for monocycle and 4-µsec chirp excitation at a repetition rate of 1 KHz.*

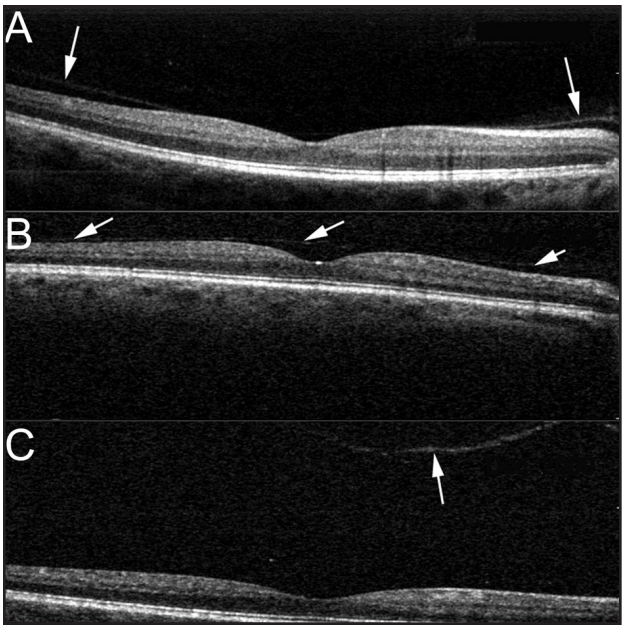


**Figure 2.** Optical coherence tomography images of the macula of the right eye obtained (A) 30 months and (B) 18 months before and (C) 1 day after symptomatic posterior vitreous detachment. At 30 months prior, the posterior hyaloid face (arrows) appears detached peripheral to the macula. At 18 months prior, the vitreous shows a shallow detachment, including over the macula. After becoming symptomatic, the vitreous is fully separated from the retinal surface in the perimacular region.

using a 40-µm aperture needle hydrophone (Model HPM04/1; Precision Acoustics, Ltd., Dorchester, UK) calibrated up to 60 MHz. Separate measurements of the acoustic field in the focal zone were made for each ring. Because only one ring (20% of the overall transducer surface area) fires at a time, the intensity at the focus would be expected to be lower than for a conventional transducer of equal overall aperture. Chirp excitation does not increase the instantaneous intensity compared with a conventional pulse, but does extend the duration of the pulse. This therefore primarily affects temporally averaged intensity and has little effect on mechanical index (which relates to cavitation risk) or instantaneous intensity. The measured intensity values were well below Food and Drug Administration 510(k) guidelines for safety for ophthalmic diagnostic ultrasound.[17]

The subject was a 59-year-old man who had experienced sudden onset of floaters in his right eye. For the right eye, K = 45.25 D @ 130 × 46.25 D @ 40 and axial length was 23.4 mm. Ophthalmoscopic examination on day 1 revealed incomplete PVD with peripheral traction, a partial-thickness retinal tear nasally, and slight vitreous hemorrhage.

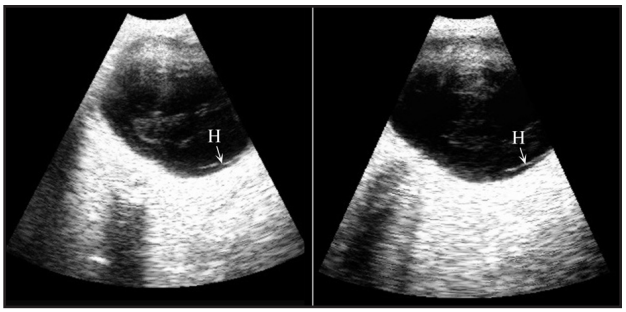


**Figure 3.** Conventional 10-MHz B-mode images obtained 1 day (left) and 3 months (right) after posterior vitreous detachment. Images are in a horizontal plane, with nasal aspect to image right. The hyaloid face (H) and kinetically mobile inhomogeneities (decreasing in brightness after 3 months) within the vitreous body can be seen in both images, but with limited detail, especially in the anterior vitreous.

OCT images (Fig. 2) acquired 30 and 18 months prior to PVD showed progressive but asymptomatic shallow, partial detachment of the vitreous in the perimacular area. OCT on day 1 showed complete detachment of the vitreous in the region of the macula. Conventional 10-MHz B-mode ultrasound (Fig. 3) acquired on day 1 and at 3 months revealed incomplete detachment of the vitreous body with a region of traction nasally.

Images were acquired with the prototype annular array 3 months after PVD. An image obtained with the array using a single 20-MHz cycle for excitation (Fig. 4) demonstrated increased resolution and depth-of-field compared with conventional 10-MHz images, but inadequate sensitivity for evaluation of the vitreous body. With chirp excitation (Fig. 5), high resolution and depth-of-field were achieved along with high sensitivity in depiction of the vitreous body.

## DISCUSSION

The transparency of the vitreous and the limited view through the pupil make optical imaging of the vitreous challenging. Although spectral-domain OCT is effective in imaging the relationship between the posterior vitreous face and the retina in the region of the macula, it is less applicable to imaging the vitreous body as a whole and regions of peripheral traction. Ultrasound can address this shortcoming, especially at the vitreoretinal interface where most probes are focused, and skilled users can generally demonstrate the posterior vitreous cortex. However, the utility of ultrasound for imaging the vitreous body as a whole is limited because of the modest resolution at 10 MHz, the limited depth-of-field of single-element probes, and reduced sensitivity at higher frequencies.

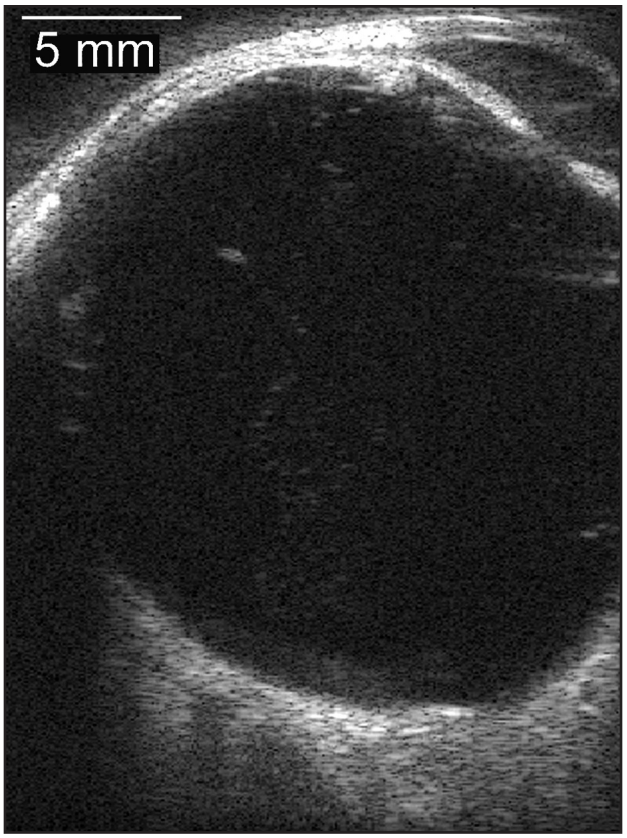


**Figure 4.** Synthetically focused image obtained with the annular array using 20-MHz monocycle excitation. Scanning was in a horizontal plane. The increased depth-of-field and the rectilinear image format resulting from linear scanning (as opposed to the more familiar sector scan common with 10-MHz probes) allows improved depiction of anterior segment structures. Nevertheless, high attenuation at 20 MHz leads to reduced sensitivity in depicting the faintly reflective structure of the vitreous body.

In this report, we described the first clinical use of a prototype 20-MHz annular array ultrasound probe for imaging the vitreous. The combination of chirp pulse encoding and synthetic focusing with an annular array addresses many shortcomings of current systems for imaging the vitreous body by providing high resolution, high sensitivity, and the capacity to image the vitreous through the overlying optically opaque structures. Although the current prototype is restricted in scan rate and uses an immersion setup, these are not inherent limitations and future real-time contact scanners are envisioned.

A capacity for real-time visualization of the vitreous body and tractional relationships with the retinal surface will play an important role in the assessment of risk for retinal detachment and for management of vitreoretinal disease.

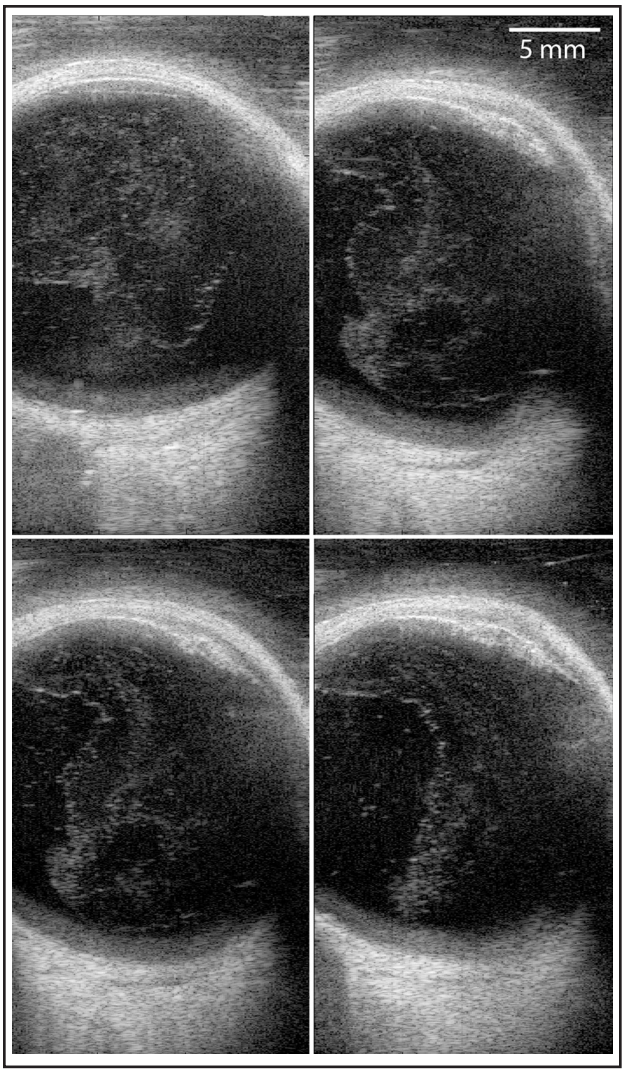


**Figure 5.** Synthetically focused images obtained using chirp excitation, with scanning in a horizontal plane avoiding the lens, nasal aspect to image right. Chirp excitation produces a significant enhancement in signal-to-noise ratio compared with monocycle excitation. The diffuse halo seen around brightly reflecting structures (vitreoretinal interface and anterior segment) is an artifact due to incomplete suppression of side lobes by the compression filter because of signal saturation.

## REFERENCES


1. Bishop PN. Structural macromolecules and supramolecular organisation of the vitreous gel. *Prog Retin Eye Res.* 2000;19:323-344.
2. Mitry D, Fleck B, Wright AF, et al. Pathogenesis of rhegmatogenous retinal detachment: predisposing factors. *Retina.* 2010;30:1561-1572.
3. Straatsma BR, Zeegen PD, Foos RY, et al. Lattice degeneration of the retina: XXX Edward Jackson Memorial Lecture. *Am J Ophthalmol.* 1974;77:619-649.
4. Oksala A. Ultrasonic findings in the vitreous body at various ages. *Graefe's Arch Clin Exp Ophthalmol.* 1978;207:275-280.
5. Weber-Kraus B, Eckardt C. Incidence of posterior vitreous detachment in the elderly. *Ophthalmologe.* 1997;94:619-623.
6. Fisher YL, Slakter JS, Friedman RA, Yannuzzi LA. Kinetic ultrasound evaluation of the posterior vitreoretinal interface. *Ophthalmology.*

1991;98:1135-1138.
7. Walton KA, Meyer CH, Harkrider CJ, et al. Age-related changes in vitreous mobility as measured by video B scan ultrasound. *Exp Eye Res*. 2002;74:173-180.
8. Hewick SA, Fairhead AC, Culy JC, Atta HR. A comparison of 10 MHz and 20 MHz ultrasound probes in imaging the eye and orbit. *Br J Ophthalmol*. 2004;88:551-555.
9. Mirza RG, Johnson MW, Jampol LM. Optical coherence tomography use in evaluation of the vitreoretinal interface: a review. *Surv Ophthalmol*. 2007;52:397-421.
10. Nigam N, Bartsch D-U G, Cheng L, et al. Spectral domain optical coherence tomography for imaging ERM, retinal edema, and vitreomacular interface. *Retina*. 2010;30:246-253.
11. Mojana F, Kozak I, Oster SF, et al. Observations by spectral-domain optical coherence tomography combined with simultaneous scanning laser ophthalmoscopy: imaging of the vitreous. *Am J Ophthalmol*. 2010;149:641-650.
12. Koizumi H, Spaide RF, Fisher YL, et al. Three-dimensional evaluation of vitreomacular traction and epiretinal membrane using spectral-domain optical coherence tomography. *Am J Ophthalmol*. 2008;145:509-517.
13. Restori M. Imaging the vitreous: optical coherence tomography and ultrasound imaging. *Eye*. 2008;22:1251-1256.
14. Mamou J, Ketterling JA, Silverman RH. Chirp-coded excitation imaging with a high-frequency ultrasound annular array. *IEEE Trans Ultrason Ferroelectr Freq Control*. 2008;55:508-513.
15. Ketterling JA, Aristizabal O, Turnbull DH, Lizzi FL. Design and fabrication of a 40-MHz annular array transducer. *IEEE Trans Ultrason Ferroelectr Freq Control*. 2005;52:672-681.
16. Ketterling JA, Ramachandran S, Aristizábal O. Operational verification of a 40-MHz annular array transducer. *IEEE Trans Ultrason Ferroelectr Freq Control*. 2006;53:623-630.
17. U.S. Food and Drug Administration. Information for Manufacturers Seeking Marketing Clearance of Diagnostic Ultrasound Systems and Transducers. http://www.fda.gov/downloads/medicaldevices/deviceregulationandguidance/guidancedocuments/ucm070911.pdf. September 9, 2008.